Original Article | Genitourinary Imaging

http://dx.doi.org/10.3348/kjr.2015.16.4.827
pISSN 1229-6929 · eISSN 2005-8330
Korean J Radiol 2015;16(4):827-834

Korean Journal of Radiology
KJR

Evaluation of Renal Oxygenation Level Changes after Water Loading Using Susceptibility-Weighted Imaging and T2* Mapping

Jiule Ding, MD[1], Wei Xing, MD[1], Dongmei Wu, MD[2], Jie Chen, MD[1], Liang Pan, MD[1], Jun Sun, MD[1], Shijun Xing, MD[1], Yongming Dai, PhD[3]

[1]Department of Radiology, Third Affiliated Hospital of Suzhou University, Changzhou, Jiangsu 213003, China; [2]Shanghai Key Laboratory of Magnetic Resonance Imaging, East China Normal University, Shanghai 200241, China; [3]Philips Healthcare, Shanghai 200000, China

Objective: To assess the feasibility of susceptibility-weighted imaging (SWI) while monitoring changes in renal oxygenation level after water loading.

Materials and Methods: Thirty-two volunteers (age, 28.0 ± 2.2 years) were enrolled in this study. SWI and multi-echo gradient echo sequence-based T2* mapping were used to cover the kidney before and after water loading. Cortical and medullary parameters were measured using small regions of interest, and their relative changes due to water loading were calculated based on baseline and post-water loading data. An intraclass correlation coefficient analysis was used to assess inter-observer reliability of each parameter. A receiver operating characteristic curve analysis was conducted to compare the performance of the two methods for detecting renal oxygenation changes due to water loading.

Results: Both medullary phase and medullary T2* values increased after water loading ($p < 0.001$), although poor correlations were found between the phase changes and the T2* changes ($p > 0.05$). Interobserver reliability was excellent for the T2* values, good for SWI cortical phase values, and moderate for the SWI medullary phase values. The area under receiver operating characteristic curve of the SWI medullary phase values was 0.85 and was not different from the medullary T2* value (0.84).

Conclusion: Susceptibility-weighted imaging enabled monitoring changes in the oxygenation level in the medulla after water loading, and may allow comparable feasibility to detect renal oxygenation level changes due to water loading compared with that of T2* mapping.

Index terms: *Magnetic resonance imaging; Blood oxygen level dependent; Susceptibility-weighted imaging; Phase; T2*; Renal oxygenation level*

INTRODUCTION

Renal oxygenation status has received considerable attention from the scientific and clinical communities (1, 2), and quantitative measurements of tissue oxygenation levels are crucial to assess tissue metabolism and function. However, the counter-current arrangement of capillary blood flow results in a state of relative hypoxia within the renal medulla under normal conditions (3), rendering the kidneys more susceptible to small changes in oxygenation level (4). Therefore, detecting oxygenation level changes in

Received July 11, 2014; accepted after revision April 8, 2015.
This work was supported by a grant from National Natural Science Foundation of China (81371513).

Corresponding author: Wei Xing, MD, Department of Radiology, Third Affiliated Hospital of Suzhou University, No.185 Juqian St, Changzhou 213003, China.
• Tel: (86519) 68870255 • Fax: (86519) 86621235
• E-mail: suzhxingwei@126.com

the kidney are clinically important, suggesting the need for non-invasive methods to measure these levels.

As T2* relaxation time is related to the deoxyhemoglobin content in tissue (5) and can be estimated from signal intensity measurements made at several different echo times, multi-echo gradient echo sequence (mGRE)-based T2* mapping is commonly used to evaluate intra-renal oxygenation level changes in animal models and humans (6-9), following the physiological or pharmacological maneuvers such as water loading (6), naproxen administration (7), and furosemide injection (8).

Susceptibility-weighted imaging (SWI) is another GRE-based method with image contrast originating from magnitude and, particularly, phase information (10). Due to the high sensitivity of its phase-to-magnetic properties, SWI serves as a quantitative method to investigate tissue oxygenation levels (10, 11). The phase takes advantage of the fact that the magnetic properties of hemoglobin depend on its oxygenation status (11). Hence, the association between phase and oxygenation status of hemoglobin enables the phase to be a possible indicator of oxygenation level. However, no studies have used SWI to evaluate renal oxygenation levels.

We hypothesized that SWI would be useful to monitor changes in renal oxygenation levels. The aim of this study was to assess the feasibility of SWI for monitoring renal oxygenation level changes after water loading.

MATERIALS AND METHODS

Subjects

This study was approved by the local Institutional Review Board, and informed consent was obtained from all subjects. The study population consisted of 32 subjects (15 females and 17 males; age range, 25–35 years; mean age, 28.0 ± 2.2 years) who met the following criteria: 1) no history of renal disease, 2) did not take any medication for up to 2 months before this study, and 3) could hold their breath for at least 15 seconds. The mean serum creatinine level was measured before a magnetic resonance imaging (MRI) examination, and was 73.72 ± 11.63 μmol/L.

The subjects were instructed to fast and stop drinking water for at least 12 hours overnight. All subjects were weighted before the MRI examination, and MRI was taken before and after water loading. MRI was carried out with the subjects in the supine position. The subjects were asked to step out from the scanner and drink 20 mL of water/kg body weight within 15 minutes for water loading. Then, they were asked to urinate every 15 minutes, and the volume of urinary eliminated was recorded. The post-water loading MRI was not taken until the volume of urine sample exceeded 75 mL every 15 minutes, indicating vigorous water diuresis and that the renal oxygenation level had changed, as shown previously (12). The second examination time depended on the urine volume of the participants. The median time interval between the two MRI examinations was 60 minutes (range, 30–90 minutes).

MRI

All MRIs were obtained on a 3.0 T whole-body system (Achieva TX, Philips Healthcare, Best, the Netherlands) equipped with a commercial 32-channel torso phase array coil. Five MRI sequences were taken in this study (Table 1).

The coronal images were used for identifying the kidneys, and all subsequent transverse images of the other sequences were acquired covering the whole kidney. The order of the

Table 1. Imaging Parameters of Magnetic Resonance Imaging Sequences

Sequences	T2WI (HASTE)	T1WI (FLASH)	T2WI (HASTE)	T2*WI (mGRE)	SWI (GRE)
Imaging plane	Coronal	Transverse	Transverse	Transverse	Transverse
Breath technique	Breath-hold	Breath-hold	Breath-hold	Breath-hold	Breath-hold
TR/TE (ms)	2400/91	161/2.46	2400/98	336/6–39.84 with a interval of 3.76	143/10
Field of view (mm^2)	380 x 380	380 x 285	380 x 285	360 x 270	360 x 270
Matrix	256 x 179	320 × 168	320 x 168	256 x 163	256 x 182
Number of slices	19	21	21	18	16
Slices thickness/gap (mm)	7.0/2.1	5.5/1.65	5.5/1.65	5.0/1.0	5.0/1.0
Flip angle (degrees)	160	70	160	60	20
Echo train length	179	-	168	-	-
Bandwidth (Hz/Px)	781	270	488	500	15

FLASH = fast low-angle shot, GRE = gradient resonance echo, HASTE = half-Fourier acquisition single-shot turbo spin echo, mGRE = multi-echo gradient resonance echo, SWI = susceptibility weighted imaging, T1WI = T1-weighted imaging, T2WI = T2-weighted imaging, T2*WI = T2*-weighted imaging, TE = echo time, TR = repeated time

Korean Journal of Radiology
KJR

transverse sequences was T1-, T2-weighted, mGRE, and SWI. Conventional T1- and T2-weighted images were used to screen the space-occupying renal lesions.

Susceptibility Weighted Imaging

Magnitude and original phase two-dimensional SWI images were produced online automatically. The original phase images were processed offline with SPIN software developed in-house (Signal Processing in NMR, Wayne State University, Detroit, MI, USA). The phase images were processed using a 32 x 32 high-pass filter (10) to remove the low frequency phase-shift artifacts caused by air-tissue interfaces and background field inhomogeneity. The phase images corrected in the previous step were acquired with pixel gray-level values of 0–4096 in the right-handed system. A simple conversion formula was used to translate the pixel-wise gray-level value to its natural range $[-\pi, \pi]$ in radians (13):

$$\text{Phase value (rad)} = \pi \left(\frac{\chi}{2048} - 1 \right) \quad (1),$$

where χ represents the measured gray-level value of the pixel, and π is 3.14.

T2* Mapping

T2* values were estimated as the slope of decay rate of the MRI signal by fitting signal intensity vs. echo-time to a single exponential function in a pixel-by-pixel scheme using SPIN software. A set of T2* maps were created and each map corresponded to a specific slice.

Imaging Analysis

All datasets were analyzed independently by two radiologists with > 10 years experience interpreting abdominal MRI. The radiologists were blinded as to whether the MRIs were obtained before or after water loading.

First, the pre- and post-water loading mGRE and SWI datasets were co-registered on an extended workstation (EWS, Philips Healthcare) to avoid mismatched artifacts resulting from different positions of the kidney image during breath holds. Then, the phase datasets were exported to SPIN for correction processing (presented in the last section) and subsequent analysis. Second, to ensure that each region of interest (ROI) fell within identifiable medullary and cortical sections, one plane through the renal hilum of each kidney was used for the image analysis at the point where the optimal contrast between the cortex and medulla was observed. The kidney ROI was divided into three segments; one cortical ROI and one medullary ROI were drawn in each segment (6–10 pixels within each ROI) and transferred to phase images and T2* maps to measure the parameters (Fig. 1). The mean phase (φ_{cortex} and $\varphi_{medulla}$), and mean T2* ($T2^*_{cortex}$ and $T2^*_{medulla}$) values were calculated by averaging the cortical and medullary ROIs, respectively, measured by the two radiologists. The relative changes (RC) in the mean phase and T2* values after water loading were calculated using the following equations.

$$RC_p = \frac{\Delta\varphi}{|\varphi_0|} \times 100\% \quad (2),$$

where RC_p is the relative change in the mean phase values; $\Delta\varphi = \varphi_1 - \varphi_0$, and φ_0 and φ_1 denote the phase values measured before and after water loading, respectively.

$$RC_t = \frac{\Delta T2^*}{|T2^*_0|} \times 100\% \quad (3),$$

where RC_t is the relative change in the mean T2* values, $\Delta T2^* = T2^*_1 - T2^*_0$, and $T2^*_0$ and $T2^*_1$ denote T2* measured

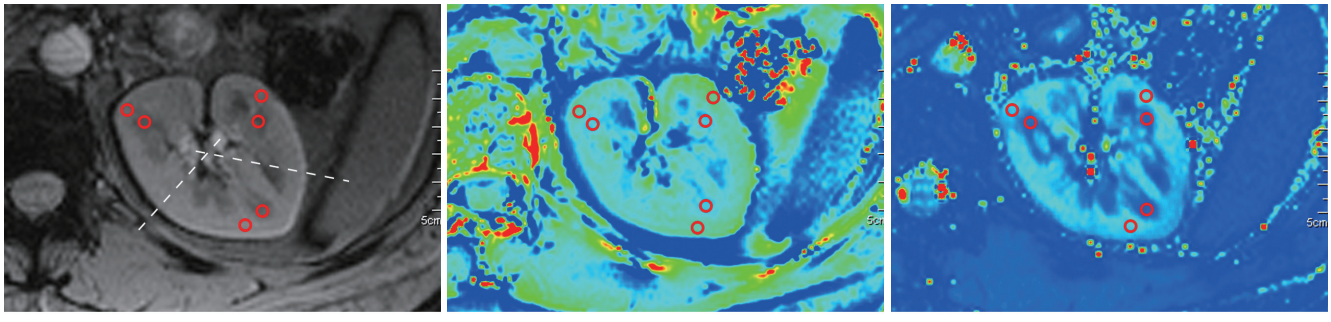

Magnitude image | Phase image | T2* map

Fig. 1. Drawing of regions of interest (ROIs) in renal parenchyma. 30-year-old male volunteer underwent transverse susceptibility-weighted imaging and T2* mapping before water loading. One cortical ROI and one medullary ROI were drawn in each segment on magnitude image and were applied to phase image and T2* map to measure parameters in cortex and medulla, respectively.

before and after water load respectively.

Statistical Analysis

Results are expressed as mean and standard deviation. The paired *t* test was used to compare the quantitative values obtained before and after water loading, and those measured by the two methods. The correlation between the phase and T2* changes was analyzed using Pearson's correlation coefficient analysis. Inter-observer reliability of each quantitative parameter was assessed using the intraclass correlation coefficient (ICC), and calculated in a two-way random effects model based on absolute agreement. In addition, the ICC computation also provided an estimate of accuracy (95% confidence interval) of the reliability levels. Agreement strengths for the ICC values were classified as follows: 0.00–0.40, poor; 0.41–0.60, moderate; 0.61–0.80, good; and 0.81–1.00, excellent correlation. The performance of the two methods for detecting renal oxygenation changes to water loading was tested using a receiver operating characteristic curve (ROC) analysis, and the areas under curves (AUC) were compared using the Z test. Sensitivity and specificity for each parameter were acquired at the same time. SPSS Statistics for Windows ver. 17.0 (SPSS Inc., Chicago, IL, USA) was used for all statistical analyses. A two-sided p value < 0.05 was considered significant.

RESULTS

Renal Oxygenation Changes due to Water Loading

After water loading, $\Delta\varphi_{cortex}$ was (1.56 ± 8.81) x 10^{-3} rad, RC_p was 1.06 ± 5.52%, and $\Delta T2^*_{cortex}$ was 0.16 ± 3.63 ms with RC_t of 0.44 ± 6.21%. No significant differences were observed for φ_{cortex} (p = 0.33) and $T2^*_{cortex}$ (p = 0.80) between pre- and post-water loading or between cortical RC_p and RC_t (p = 0.68). In contrast, $\Delta\varphi_{medulla}$ was (3.05 ± 2.05) x 10^{-3} rad, RC_p was 26.07 ± 15.52%, $\Delta T2^*_{medulla}$ was 2.58 ± 1.30 ms, and RC_t was 10.45 ± 5.46%. Significant differences were detected for $\varphi_{medulla}$ and $T2^*_{medulla}$ after water loading (p < 0.001), and between medullary RC_p and RC_t (p < 0.001) (Fig. 2).

Correlations between the Phase Changes and T2* Changes

No positive linear correlations were detected between the phase changes and the T2* changes due to water loading (all

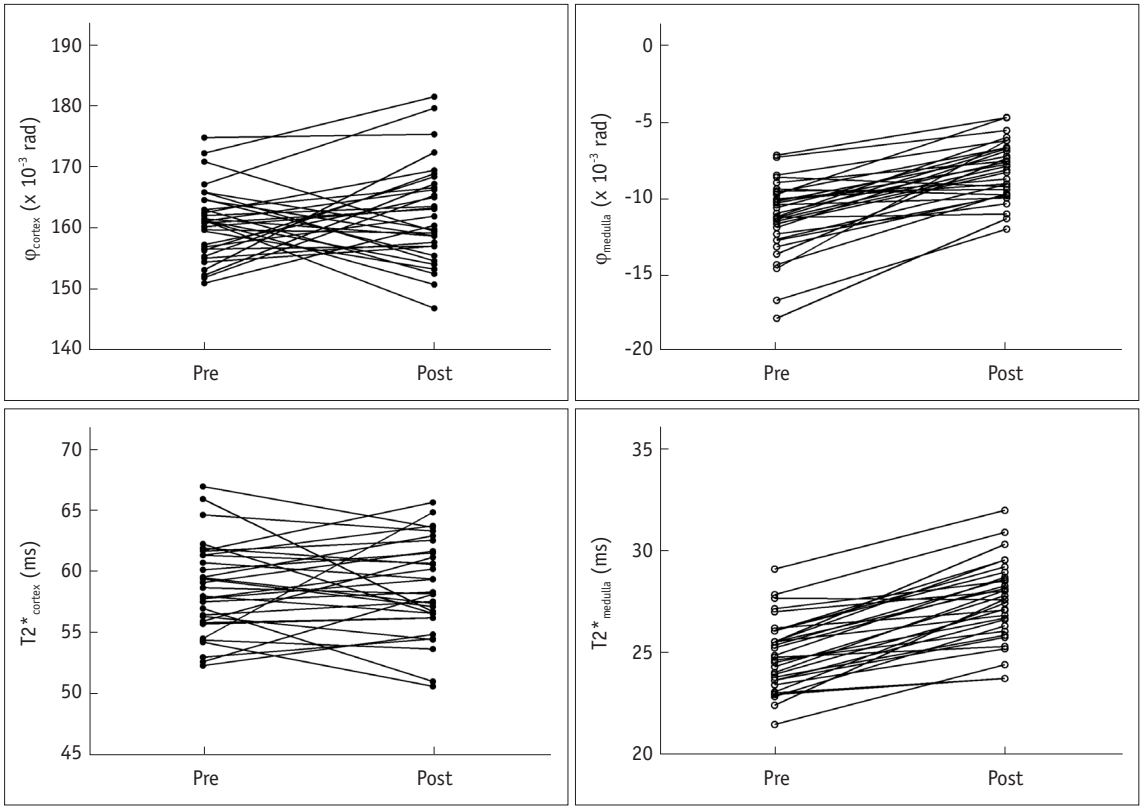

Fig. 2. Distinct change in trend of quantitative parameter measurements appeared in renal medulla after water loading. Very few changes in phase and T2* values occurred in renal cortex, whereas medullary values increased for most of subjects after water loading.

Korean Journal of Radiology
KJR

$p > 0.05$) (Fig. 3).

Interobserver Reliability

Interobserver reliability was excellent for the T2* values, followed by φ_{cortex} and $\varphi_{medulla}$ (Table 2).

Comparison of the Two Methods by ROC Analysis

The AUC was 0.85 for $\varphi_{medulla}$ and 0.84 for $T2^*_{medulla}$ (p = 0.85) (Fig. 4). Sensitivity and specificity were 87.50% and 71.87%, respectively when the $\varphi_{medulla}$ cutoffs was -9.99 x 10^{-3} rad, 75.00%, and 84.40% respectively when the $T2^*_{medulla}$ cutoff was 26.22 ms.

DISCUSSION

Blood flow supplied to the renal cortex normally far exceeds the metabolic needs of the renal cortex, whereas the renal medulla is short of blood supply and relatively hypoxic (3). Therefore, the kidney is actually two organs of the cortex and medulla in terms of oxygenation level (3). A previous study used invasive microelectrodes and demonstrated a significant gradient in tissue oxygenation within the kidney (14). The two methods used here detected lower phase and T2* values in the renal medulla compared to those of renal cortex pre- and post-water loading, suggesting that both methods detected the oxygenation difference between the cortex and medulla.

Cortical oxygenation was higher and insensitive to water

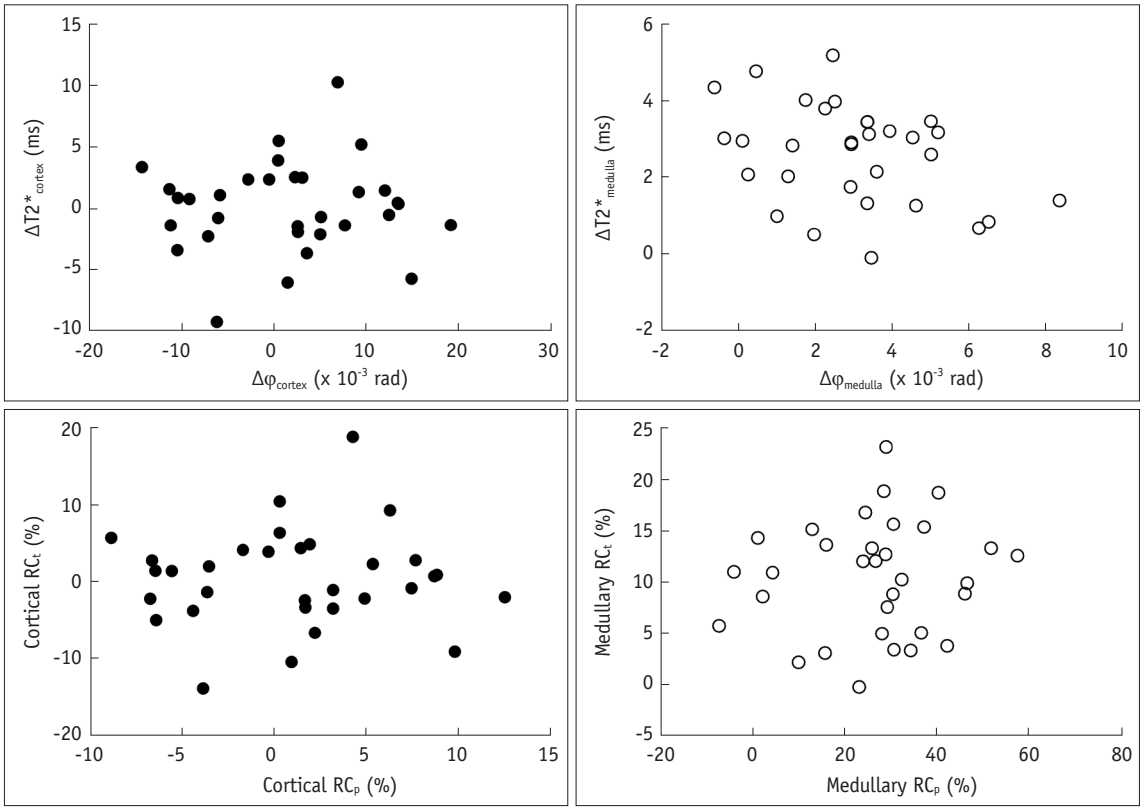

Fig. 3. Correlations between phase changes and T2* changes due to water loading. Poor correlations were present between phase changes and T2* changes (all $p > 0.05$).

Table 2. Interobserver Reliability Level of Phase and T2* Values (n = 32)

Groups		Phase Values (x 10^{-3} Rad)		ICC (95% CI)	T2* Values (ms)		ICC (95% CI)
		Radiologist 1	Radiologist 2		Radiologist 1	Radiologist 2	
Pre	Cortex	163.64 ± 7.92	158.36 ± 7.73	0.79 (0.23, 0.94)	59.25 ± 5.27	58.12 ± 6.19	0.94 (0.80, 0.98)
	Medulla	-11.22 ± 2.34	-11.15 ± 3.88	0.60 (-0.30, 0.88)	26.00 ± 2.42	23.86 ± 2.44	0.85 (0.48, 0.96)
Post	Cortex	163.67 ± 11.41	161.44 ± 11.94	0.75 (0.07, 0.93)	59.28 ± 5.22	58.41 ± 5.79	0.95 (0.82, 0.99)
	Medulla	-8.34 ± 2.03	-7.93 ± 2.69	0.50 (-0.80, 0.86)	28.85 ± 3.06	26.16 ± 2.06	0.83 (0.42, 0.95)

Data was represent as mean and standard deviation. CI = confidence interval, ICC = intraclass correlation coefficient

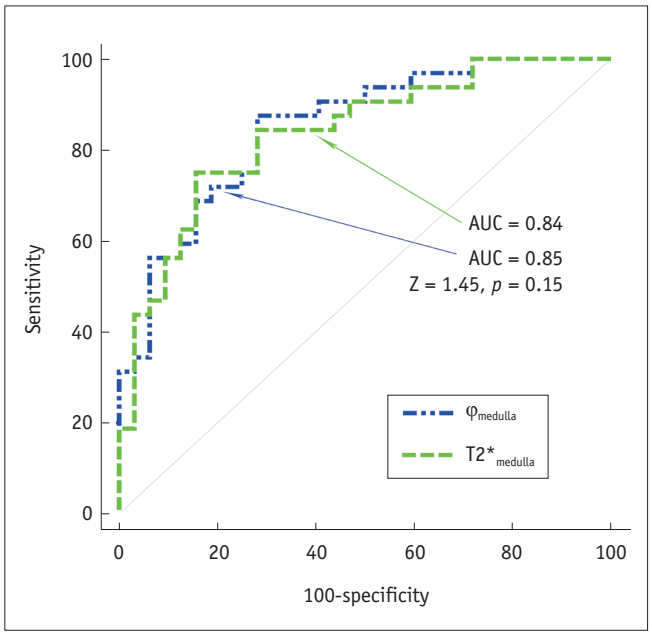

Fig. 4. Receiver operating characteristics curve analysis of two methods for detecting changes in renal oxygenation levels due to water loading. Area under receiver operating characteristic curve (AUC) was not significantly larger for medullary phase ($\varphi_{medulla}$), as measured using susceptibility weighted imaging, than medullary T2* values ($T2^*_{medulla}$) using T2* map.

loading. In this study, the cortical T2* and phase values were not different after water loading. The oxygenation status of the cortex in a normal kidney found in this study was consistent with that reported previously (6, 15). Unlike the renal cortex, medullary oxygenation is sensitive to water loading. The tonic endogenous prostaglandin (PGE_2) contributes to decrease deoxyhemoglobin levels in the renal medulla after water loading in young subjects (16). In other words, the decrease in deoxyhemoglobin level results from the reduced consumption of oxygen as indicated by the increased phase (26.1%) and T2* (10.4%) values within the medulla after water loading.

Both the phase and T2* values are affected by the concentrations of components, such as iron and deoxyhemoglobin (17-20). Phase and T2* values have been used in previous studies to quantify putative iron content in the human brain, and the results of both methods had good agreement in some structures but poor agreement in others (21, 22). In another study that quantified hepatic iron deposition in patients with cirrhosis, the phase and T2* values were linearly correlated with serum ferritin concentrations, and a positive correlation was found between the two methods for patients but not for healthy individuals (23). We found no correlation between the phase changes and T2* changes in healthy volunteers.

The lack of a correlation between the two methods in our study can be attributed to different signal change mechanisms. In a previous study on iron deposition in the brain (24), large amounts of iron, which cause strong dephasing across a voxel, cause appropriate decreases in T2*, whereas smaller amounts of iron, which cause weaker dephasing across a voxel, may have little effect on T2*. Hence, phase is much more sensitive to lower iron concentrations, and phase aliasing occurs when iron content is too high (24), which may be the reason why the phase change was double that of the T2* changes in the renal medulla due to water loading. Similarly, we deduced that the different signal change mechanics of both methods were responsible for the lack of a correlation in our results, as oxyhemoglobin possesses diamagnetic properties. Therefore, both phase and T2* mapping have their advantages when the exact deoxyhemoglobin concentration is unknown.

Notably, the orientation of the kidney in a magnetic field can affect the phase measurement. For example, phase shifts depend on the orientation of the underlying white matter fibers with respect to the main magnetic field *in vivo* (25). Renal parenchyma has a well-defined structure consisting of tubules, collecting ducts, and vessels oriented radially from the cortex towards the pelvis, which can be observed microscopically. In particular, diffusion tensor imaging reveals highly structured tine tubules and vessels delicately arranged in the renal medulla (26, 27). In this study, we assumed that the highly structured renal tissue may have affected the phase measurements, and that the adverse influence was minimized by selecting slices through the renal hilum where structured tine tubules and vessels for each kidney of the volunteers were related vertically with the main magnetic axis (z-axis).

This study had several limitations that should be recognized. First, the renal oxygenation level changes due to water loading detected by phase changes were confirmed by T2* mapping, but the golden standard of invasive microelectrodes was not used on healthy volunteers. The renal tissue oxygenation changes measured by SWI should be confirmed using an invasive probe in an animal study (28) or by the urine or serum oxidative stress biomarkers in human studies as indicated previously (29). Second, quantitative susceptibility mapping could be an attractive post-processing technique to better quantify oxygenation levels, but this technique requires higher resolution than that used in this study (30). Third, we used consecutive breath hold acquisitions for the kidney

Korean Journal of Radiology
KJR

coverage measurements, which may not be feasible when this technique is applied to patients with a deteriorated respiratory condition. Fourth, even with high-pass filters and image co-registration of the phase images, extra-phase errors can be introduced due to different field inhomogeneities at two separate measurements for each volunteer before and after water loading, which may have adversely affected the accuracy of the quantitative analysis.

In conclusion, our study was the first to demonstrate changes in renal oxygenation levels after water-load using both SWI and T2* mapping. SWI phase images were used to monitor changes in oxygenation levels in the renal medulla after water loading, and the results were confirmed by T2* mapping, indicating that SWI may be adequate to detect renal oxygenation level changes after water loading, similar to T2* mapping.

REFERENCES

1. Brezis M, Rosen S. Hypoxia of the renal medulla--its implications for disease. *N Engl J Med* 1995;332:647-655
2. Eckardt KU, Bernhardt WM, Weidemann A, Warnecke C, Rosenberger C, Wiesener MS, et al. Role of hypoxia in the pathogenesis of renal disease. *Kidney Int Suppl* 2005;(99):S46-S51
3. Epstein FH, Agmon Y, Brezis M. Physiology of renal hypoxia. *Ann N Y Acad Sci* 1994;718:72-81; discussion 81-82
4. Zhang W, Edwards A. Oxygen transport across vasa recta in the renal medulla. *Am J Physiol Heart Circ Physiol* 2002;283:H1042-H1055
5. Li LP, Vu AT, Li BS, Dunkle E, Prasad PV. Evaluation of intrarenal oxygenation by BOLD MRI at 3.0 T. *J Magn Reson Imaging* 2004;20:901-904
6. Tumkur SM, Vu AT, Li LP, Pierchala L, Prasad PV. Evaluation of intra-renal oxygenation during water diuresis: a time-resolved study using BOLD MRI. *Kidney Int* 2006;70:139-143
7. Ji L, Li LP, Schnitzer T, Du H, Prasad PV. Intra-renal oxygenation in rat kidneys during water loading: effects of cyclooxygenase (COX) inhibition and nitric oxide (NO) donation. *J Magn Reson Imaging* 2010;32:383-387
8. Li LP, Storey P, Pierchala L, Li W, Polzin J, Prasad P. Evaluation of the reproducibility of intrarenal R2* and Delta R2* measurements following administration of furosemide and during waterload. *J Magn Reson Imaging* 2004;19:610-616
9. Li LP, Ji L, Lindsay S, Prasad PV. Evaluation of intrarenal oxygenation in mice by BOLD MRI on a 3.0T human whole-body scanner. *J Magn Reson Imaging* 2007;25:635-638
10. Haacke EM, Xu Y, Cheng YC, Reichenbach JR. Susceptibility weighted imaging (SWI). *Magn Reson Med* 2004;52:612-618
11. Haacke EM, Tang J, Neelavalli J, Cheng YC. Susceptibility mapping as a means to visualize veins and quantify oxygen saturation. *J Magn Reson Imaging* 2010;32:663-676
12. Zuo CS, Rofsky NM, Mahallati H, Yu J, Zhang M, Gilbert S, et al. Visualization and quantification of renal R2* changes during water diuresis. *J Magn Reson Imaging* 2003;17:676-682
13. Wu Z, Mittal S, Kish K, Yu Y, Hu J, Haacke EM. Identification of calcification with MRI using susceptibility-weighted imaging: a case study. *J Magn Reson Imaging* 2009;29:177-182
14. Aukland K, Krog J. Renal oxygen tension. *Nature* 1960;188:671
15. Han F, Xiao W, Xu Y, Wu J, Wang Q, Wang H, et al. The significance of BOLD MRI in differentiation between renal transplant rejection and acute tubular necrosis. *Nephrol Dial Transplant* 2008;23:2666-2672
16. Prasad PV, Epstein FH. Changes in renal medullary pO2 during water diuresis as evaluated by blood oxygenation level-dependent magnetic resonance imaging: effects of aging and cyclooxygenase inhibition. *Kidney Int* 1999;55:294-298
17. Ning N, Zhang L, Gao J, Zhang Y, Ren Z, Niu G, et al. Assessment of iron deposition and white matter maturation in infant brains by using enhanced T2 star weighted angiography (ESWAN): R2* versus phase values. *PLoS One* 2014;9:e89888
18. Yan SQ, Sun JZ, Yan YQ, Wang H, Lou M. Evaluation of brain iron content based on magnetic resonance imaging (MRI): comparison among phase value, R2* and magnitude signal intensity. *PLoS One* 2012;7:e31748
19. Li M, Hu J, Miao Y, Shen H, Tao D, Yang Z, et al. In vivo measurement of oxygenation changes after stroke using susceptibility weighted imaging filtered phase data. *PLoS One* 2013;8:e63013
20. Neugarten J. Renal BOLD-MRI and assessment for renal hypoxia. *Kidney Int* 2012;81:613-614
21. Aquino D, Bizzi A, Grisoli M, Garavaglia B, Bruzzone MG, Nardocci N, et al. Age-related iron deposition in the basal ganglia: quantitative analysis in healthy subjects. *Radiology* 2009;252:165-172
22. Yao B, Li TQ, Gelderen Pv, Shmueli K, de Zwart JA, Duyn JH. Susceptibility contrast in high field MRI of human brain as a function of tissue iron content. *Neuroimage* 2009;44:1259-1266
23. Tao R, Zhang J, Dai Y, You Z, Fan Y, Cui J, et al. An in vitro and in vivo analysis of the correlation between susceptibility-weighted imaging phase values and R2* in cirrhotic livers. *PLoS One* 2012;7:e45477
24. Haacke EM, Miao Y, Liu M, Habib CA, Katkuri Y, Liu T, et al. Correlation of putative iron content as represented by changes in R2* and phase with age in deep gray matter of healthy adults. *J Magn Reson Imaging* 2010;32:561-576
25. Liu C, Li W, Wu B, Jiang Y, Johnson GA. 3D fiber tractography with susceptibility tensor imaging. *Neuroimage* 2012;59:1290-1298
26. Ries M, Jones RA, Basseau F, Moonen CT, Grenier N. Diffusion tensor MRI of the human kidney. *J Magn Reson Imaging*

2001;14:42-49
27. Sigmund EE, Vivier PH, Sui D, Lamparello NA, Tantillo K, Mikheev A, et al. Intravoxel incoherent motion and diffusion-tensor imaging in renal tissue under hydration and furosemide flow challenges. *Radiology* 2012;263:758-769
28. Raman JD, Bensalah K, Bagrodia A, Tracy CR, Kabbani W, Sagalowsky AI, et al. Comparison of tissue oxygenation profiles using 3 different methods of vascular control during porcine partial nephrectomy. *Urology* 2009;74:926-931
29. Djamali A, Sadowski EA, Muehrer RJ, Reese S, Smavatkul C, Vidyasagar A, et al. BOLD-MRI assessment of intrarenal oxygenation and oxidative stress in patients with chronic kidney allograft dysfunction. *Am J Physiol Renal Physiol* 2007;292:F513-F522
30. Li J, Chang S, Liu T, Wang Q, Cui D, Chen X, et al. Reducing the object orientation dependence of susceptibility effects in gradient echo MRI through quantitative susceptibility mapping. *Magn Reson Med* 2012;68:1563-1569